Ballistic electron transport in thin silicon dioxide films

M. V. Fischetti, D. J. DiMaria, L. Dori, J. Batey, E. Tierney, and J. Stasiak
IBM Thomas J. Watson Research Center, P.O. Box 218, Yorktown Heights, New York 10598
(Received 4 November 1986)

Electron transport in thin (3.8—5.8-nm) silicon dioxide films has been investigated with use of the carrier-separation and vacuum-emission techniques. For the thinner films and smaller voltages, ballistic transport is inferred not only *indirectly* from the oscillations of the current-voltage characteristics (as originally reported by Lewicki and Maserjian) but also *directly* from the average energy measured via the carrier-separation technique and from the observation of the ballistic peak (about 0.15 eV wide) in the vacuum-emission experiments. In thicker films and/or at higher bias voltages, the transition from the ballistic to the steady-state regime is observed. Phonon replicas for the 0.153- and 0.063-eV longitudinal optical phonons have been observed in this transient situation. The experimental results have been compared to Monte Carlo simulations. Best agreement has been obtained by using a value of $0.7m_0$ for the polaron mass. The average mean free path of about 1 nm resulting from the simulation is in good agreement with Lewicki and Maserjian's experimental data.

I. INTRODUCTION

One of the most spectacular results of the interplay between basic science and technology is provided by the recent observation of ballistic electron transport in semiconductors. So far these observations have been confined to III-V compound semiconductors,[1,2] mainly because the low electron-phonon scattering rates exhibited by these small-effective-mass materials translate into electron mean free paths which are comparable to the minimum dimensions technologically obtainable today. Recent results indicate that collision processes other than polar electron-phonon scattering dominate the transport in the highly doped regions of the so-called "ballistic devices." Namely, electrons lose their ballistic behavior by exciting collective coupled plasmon-phonon modes of the electron-gas—lattice system in the transit region.[3,4] Thus, a simple correlation between electron-lattice scattering parameters and experimental data is hampered by a more complex physical picture.

In this paper we present results about ballistic transport in thin films of silicon dioxide. These results are important from a practical point of view, since it is obvious that the microelectronics technology needs a better understanding of electron transport in these films. The thickness of the gate oxides used in field-effect transistors (FET's) is now approaching the 10-nm limit in the production environment and layers as thin as 4 nm are expected to be employed in the devices of the 1990s. Hot electrons intentionally or accidentally injected into the gate insulator are commonly blamed for the reduced reliability of these films and we must understand in full detail how they lose their energy if we want to gain better control of the technology. From the perspective of fundamental research, SiO_2-based systems provide a direct test of transport theories. Some of our results replicate the observations made in the III-V compounds, if we account for the shorter electron mean free path in SiO_2—which is due to both the higher effective mass ($0.067m_0$ in GaAs, $0.5m_0$ in SiO_2, m_0 being the free-electron mass) and to the different dielectric constant—and for the amorphous structure of the SiO_2. In addition, thanks to the low concentration of free carriers in SiO_2 even at the highest densities of injected current, the thermalizing and broadening electron-electron interaction is virtually absent in this system. Thus, individual electron-phonon collisions are observable in the form of sidebands (or "phonon replicas") in the electron distributions, and detailed information about the electron-phonon interaction can be directly obtained from the experimental data.

We have presented some of these results in a previous Letter.[5] Here we want to give a more-detailed presentation of our work. We proceed as follows. In Sec. II we discuss the oscillations which are observable in the current-voltage characteristics of metal-oxide-semiconductor (MOS) structures when electrons tunnel through the insulators. These oscillations have been attributed to the quantum reflections that ballistic electrons suffer at the sharp potential discontinuity of the SiO_2-electrode interface. To our knowledge, at the time this was observed and correctly interpreted by Lewicki and Maserjian,[6] it constituted the first evidence of ballistic transport in condensed matter. We present additional support to this interpretation by showing (1) that much weaker but clear reflections occur also at the SiO_2-Al and SiO_2—polycrystalline-Si interfaces, and (2) that the amplitude of the oscillations (also when observed at low temperature and with an external magnetic field) is quantitatively consistent with the strength of the electron—LO-phonon interaction in SiO_2. In Sec. III we describe the carrier-separation experiments[7] and show directly that below 4 V of applied bias most of the electrons which have tunneled through the oxide will travel ballistically in the remaining portion of the insulator. In Sec. IV we describe data related to the vacuum-emission experiments.[8] They show the shift and decay of the ballistic electron peak as the gate voltage is increased and the occurrence of satellite peaks as the ballistic electrons lose en-

ergy to one or two LO phonons. These data constitute an excellent test for the parameters entering the Monte Carlo simulations we have employed to explain the data. The excellent agreement between the experimental data (obtained in amorphous films) and the simulations (which treat the oxide as a perfect crystal) will lead us in Sec. V to some speculations about the short-range order of thermally grown SiO_2 films.

II. OSCILLATIONS OF THE TUNNELING CURRENT

In 1974 Lewicki and Maserjian[6] began a systematic study of the current-voltage characteristics of MOS capacitors in the Fowler-Nordheim tunneling regime. The main motivation of their work was the analysis of the E-vs-k dispersion relation for electrons in the forbidden gap of SiO_2. Their careful evaluation of the tunneling current brought them beyond the usual Wentzel-Kramers-Brillouin (WKB) approximation. The exact numerical solution of the Schrödinger equation describing electrons tunneling through a trapezoidal (direct tunneling) or triangular (Fowler-Nordheim tunneling) barrier had been given by Gundlach.[9] His analysis showed that for a barrier with sharp potential steps quantum interference effects resulted from reflections of the electron wave functions at the sharp potential discontinuity. As in every interference effect, phase coherence is a necessary requirement for the phenomenon to occur. Thus, two effects might prevent the observation of the predicted "quantum oscillations:" (1) phase-destroying inelastic electron-phonon collisions for electrons traveling in the SiO_2 conduction band after having tunneled through the forbidden gap[6] and (2) roughness at SiO_2 electrodes (Si substrate or metal-polysilicon gate) interfaces which could randomize the phase of the ballistic electrons emerging in the anode and average out to zero the amplitude of the oscillations.[10] The observation of the oscillations proved the existence of ballistic electrons across distances of the order of 2 to 3 nm in the SiO_2 conduction band. The asymmetry of the oscillations (not reported by Lewicki and Maserjian for tunneling through the oxide into the metal-gate—SiO_2 interface) proved that the Si-SiO_2 interface is much more smooth and abrupt at the atomic scale than the metal-SiO_2 interface. This last observation is usually accounted for by considering the high degree of chemical reactivity with SiO_2 exhibited by most of the metals used as gate materials, such as Al, Cr, Ni, or Mg. From the decay of the oscillations as the distance the electrons travel in the SiO_2 conduction band increases (either by increasing the oxide thickness or by increasing the gate voltage), a value of about 0.65 nm was deduced[11] for the inelastic mean free path of electrons in SiO_2. At the time, this was a controversial conclusion, as other models predicted much smaller values (around 0.1 or 0.2 nm).[12]

In previous publications,[13,14] we have shown that mean free paths of the magnitude inferred by Lewicki and Maserjian are actually consistent with both experimental and theoretical results concerning high-field, steady-state electron transport in SiO_2. To handle the transient regime occurring in the tunneling experiments just mentioned, we have replicated and extended the original experiments and have confirmed our results with Monte Carlo simulations.

Figure 1 shows the tunneling current-voltage characteristics for a polysilicon-gate, p-channel field-effect transistor (FET) with a gate oxide 3.85 nm thick. The Fowler-Nordheim fit to the data is shown by the solid line. The quantum oscillations are clearly visible.

From the exact integration of the Schrödinger equation, Gundlach obtained an algebraically complicated expression for the transmission probability P across the insulator as a function of the field F applied to the barrier.[9] Referring to Fig. 2 and considering the case of injection from the metal gate of an electron at the Fermi energy E_F, this is

$$P(F)=\frac{k_s}{k_m}\frac{4}{\pi^2}\left[\left[\frac{\beta}{k_m}[\mathrm{Ai}'(\beta x_t)\mathrm{Bi}'(-\beta x_L)-\mathrm{Ai}'(-\beta x_L)\mathrm{Bi}'(\beta x_t)]+\frac{k_s}{\beta}[\mathrm{Ai}(\beta x_t)\mathrm{Bi}(-\beta x_L)-\mathrm{Ai}(-\beta x_L)\mathrm{Bi}(\beta x_t)]\right]^2+\left[\frac{k_s}{k_m}[\mathrm{Ai}(-\beta x_L)\mathrm{Bi}'(\beta x_t)-\mathrm{Ai}'(\beta x_t)\mathrm{Bi}(-\beta x_L)]+[\mathrm{Ai}(\beta x_t)\mathrm{Bi}'(-\beta x_L)-\mathrm{Ai}'(-\beta x_L)\mathrm{Bi}(\beta x_t)]\right]^2\right]^{-1}, \tag{1}$$

where e is the magnitude of the electron charge, ϕ_x (ϕ_m) is the potential barrier at the oxide-silicon (oxide-metal) interface, $k_m=(2m_mE_F)^{1/2}/\hbar$ is the electron wave vector in the metal with effective mass m_m, $k_s=[2m_s(\phi_s+eFx_L)]^{1/2}/\hbar$ is the wave vector in the silicon substrate with electron effective mass m_s, $x_t=\phi_m/eF$ is the tunneling distance in the insulator, $x_L=d-x_t$ is the distance the electrons travel in the SiO_2 conduction band after having tunneled, d is the oxide thickness, $\beta=(2m_{ox}eF/\hbar^2)^{1/3}$, m_{ox} is the effective mass in the SiO_2 band gap (assumed to be constant), and, finally, $\mathrm{Ai}(x)$ and $\mathrm{Bi}(x)$ are the Airy functions and $\mathrm{Ai}'(x)$ and $\mathrm{Bi}'(x)$ their derivatives.

To enhance the "detection" of the quantum oscillations, we show in Fig. 3 the ratio J/J_{FN} of the measured current density J over the Fowler-Nordheim fit to the data, J_{FN}, as a function of the potential drop $\Delta V=V_{ox}-\phi_B/e$ (where ϕ_B is the potential barrier at the cathode-SiO_2 interface, i.e., the barrier ϕ_m in this case) across the distance x_L in the oxide. Since this quantity will be used several times in the following, it should be kept in mind that $e\Delta V$ is the maximum kinetic energy

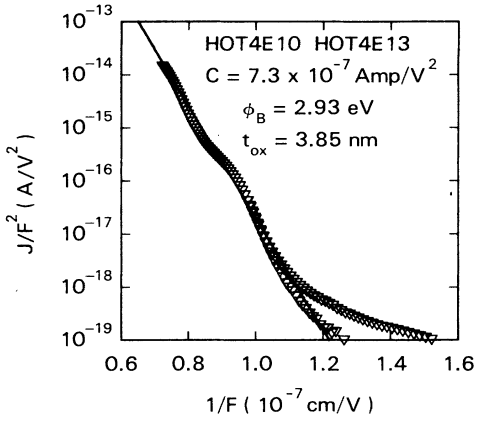

FIG. 1. Fowler-Nordheim plot of the current density J of electrons tunneling through the gate oxide of two polysilicon-gate, p-channel FET's at negative gate bias. F is the electric field applied to the oxide. The straight line is the least-squares fit to the data using the WKB Fowler-Nordheim expression $J/F^2=C\exp(-2\gamma)$, with $\gamma=2(2m_{ox})^{1/2}\phi_B^{3/2}/(3e\hbar F)$. The value of ϕ_B shown is obtained using the value $m_{ox}=0.5m_0$ given in Ref. 22, and it is consistent with the barrier expected for tunneling from the quantum levels in the Si accumulation layer. The quantum oscillations—due to reflections of ballistic electrons at the Si-SiO_2 interface—are clearly visible.

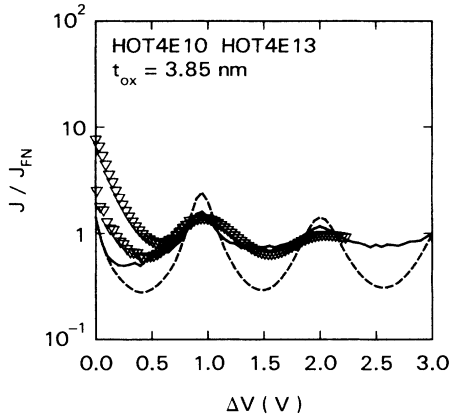

FIG. 3. The ratio of the experimental current density J of the samples considered in Fig. 1 to the Fowler-Nordheim fit J_{FN} (open triangles) as compared to the theoretical ratio P/P_{WKB} given by Eqs. (1) and (2) of the text expected for pure ballistic transport (dashed line) and corrected for the fraction of electrons reaching ballistically the oxide-anode interface (solid line), given by Eq. (3) of the text. The oxide thickness is determined from the period of the oscillations.

(measured from the bottom of the SiO_2 conduction band) an electron can have when emerging into the collecting electrode (i.e., the anode). We compare the experimental curve with the theoretical ratio P/P_{WKB} where P is the exact tunneling probability given by Eq. (1) and P_{WKB} is its WKB approximation:[15]

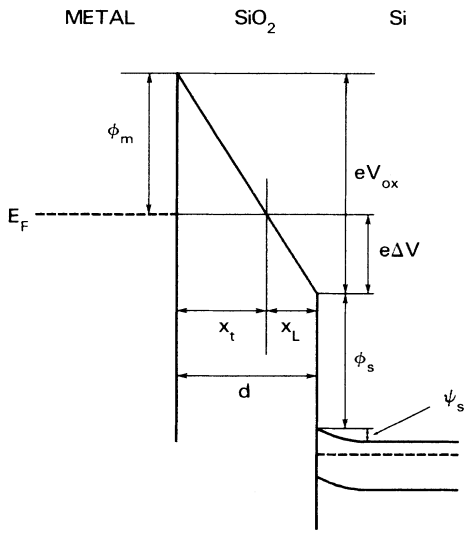

FIG. 2. Schematic band diagram of a metal-gate MOS capacitor with the gate negatively biased illustrating the quantities employed in Eqs. (1) and (2) of the text.

$$P_{WKB}=\frac{16k_s\exp(-2\gamma)}{k_m(b/a+ab/k_m^2+k_s^2/ab+ak_s^2/bk_m^2)}\ , \tag{2}$$

where $\gamma=2(2m_{ox})^{1/2}\phi_m^{3/2}/(3e\hbar F)$, $a=(2m_{ox}\phi_m)^{1/2}\hbar$, and $b=(2m_{ox}eFx_L)^{1/2}/\hbar$. We have already mentioned the two main reasons why the observed amplitude of the oscillations is smaller than predicted: electron-phonon inelastic collisions in the oxide and nonabruptness of the anode-SiO_2 interface. A third possibility originates from the fact that in real experiments the energy distribution of the injected electrons has a finite width, so that a further smearing of the oscillations might result from taking the average over the initial electron energy. However, when injecting from the polysilicon gate, quantization effects in the accumulation layer[16] may give a narrower distribution than in the case of injection from a metal electrode considered in Ref. 6. Thus, we have ignored this source of broadening of the oscillations. More important, a final source of complications comes from the fundamental problem of how to match the electronic wave functions at the interfaces between different solids: The expression for P given by Eq. (1) has been obtained by imposing the continuity of the wave functions ψ and the associated group velocities $(d\psi/dx)/m_{eff}$ (m_{eff} being the electron effective mass in the two materials) across the interfaces. In general, this will allow conservation of probability current but not necessarily conservation of crystal momentum if we account for the different band structure of the two solids. A more accurate transfer-matrix approach would be necessary. In addition, the wave vectors k_m and k_s depend on the band structures of the contacts (Si substrate and gate) via the position of the Fermi level and the electron group velocities. We have assumed the same values used by Powell,[17] since they fit internal photoemission data reasonably well. Given the uncertainty of these pa-

rameters and the problems associated with the choice of the boundary conditions, we have taken a semiempirical approach by assuming that the Si-SiO_2 interface is abrupt within a few tenths of 1 nm (consistent with the results of Refs. 10 and 18), so that the amplitude of the oscillations is only marginally affected by the "shape" of the potential discontinuity. The amplitude of the oscillations is then modulated only by the fraction of the electrons which reach the Si-SiO_2 interface without suffering any collisions. Similarly, the period becomes a sole function of the oxide thickness which we determine by fitting the data with the period predicted by Eq. (1). Typically, this determination of the oxide thickness agrees within better than 0.2 nm with the results from ellipsometry measurements. The solid curve of Fig. 3 is obtained by simulating with a Monte Carlo technique[13,14] the transport of $n_{\rm tot}$ electrons through the oxide, counting the number $n_{\rm bal}$ of the electrons reaching the contact ballistically, and obtaining the "weighted" relative amplitude

$$\frac{J}{J_{\rm FN}}=\frac{(n_{\rm tot}-n_{\rm bal})+n_{\rm bal}P/P_{\rm WKB}}{n_{\rm tot}} . \tag{3}$$

Low-energy electrons, such as those considered here, interact with the SiO_2 mainly via the polar interaction with the longitudinal-optical (LO) phonons, while nonpolar scattering with optical and acoustic phonons becomes significant at electron energies larger than about 2 eV (Refs. 13 and 14). The dimensionless coupling constant α between electrons and LO phonons is given to first order in the usual Fröhlich Hamiltonian by[14]

$$\alpha=\frac{e^2}{8\pi\hbar\omega_{\rm LO}}\left[\frac{2m^*\omega_{\rm LO}}{\hbar}\right]^{1/2}\left[\frac{1}{\epsilon_>}-\frac{1}{\epsilon_<}\right] , \tag{4}$$

where e is the magnitude of the electron charge, m^* is the electron effective mass at the bottom of the SiO_2 conduction band, $\epsilon_>$ ($\epsilon_<$) is the dielectric constant at a frequency higher (lower) than the frequency $\omega_{\rm LO}$ of the LO phonon, where we have considered two LO phonons with energies $\hbar\omega_{\rm LO}=0.063$ and 0.153 eV (Refs. 19 and 20). The values of the dielectric constant for SiO_2 are well established.[19] On the contrary, a source of uncertainty for the determination of the scattering rate at low energy might still be the value of the electron effective mass m^*. This uncertainty stems from fundamental questions concerning the time needed by the electrons to be "dressed" by the optical phonons to form a polaron, whether this occurs during the tunneling process, and how the interference phenomena discussed in the preceding section affect the tunneling and transit time of the carriers. Therefore, we have treated m^* as an adjustable parameter and have used the polaron mass[21] $m_{\rm pol}=m^*(1-\alpha/6)$ ($\simeq 1.35m^*$ accounting for the two LO phonons) as "inertial" mass for the electrons in the Monte Carlo simulation at low energy ($\lesssim 2$ eV), while the free-electron mass has been employed at energies exceeding 5 eV, as described in our previous publications.[13,14] A linear interpolation for both the effective mass as well as the nonpolar scattering rates has been employed in the intermediate energy range, and we shall see in the following sections the effect of these approximations. We have then found the best fit to the data shown

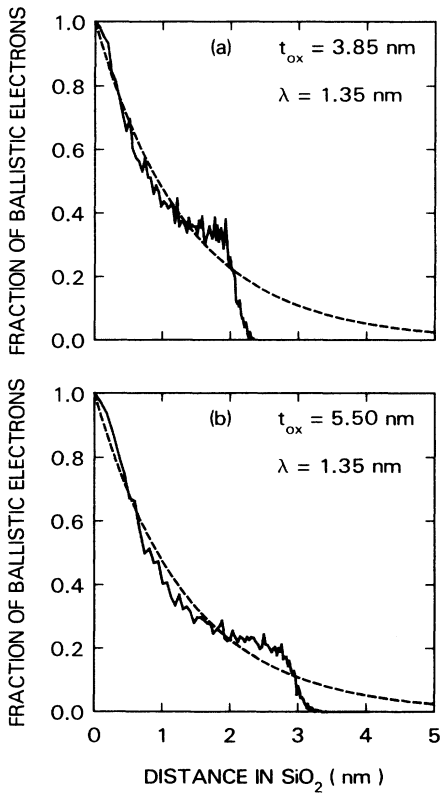

FIG. 4. Fraction of ballistic electrons reaching the oxide-anode interface as obtained from Monte Carlo simulations for two oxide thickness. The dashed lines are empirical exponential fits to the data providing the value of the "effective" mean free path λ shown. Notice that the electric field is constantly varied to simulate experimentally the conditions met during Fowler-Nordheim injection under an increasing electric field.

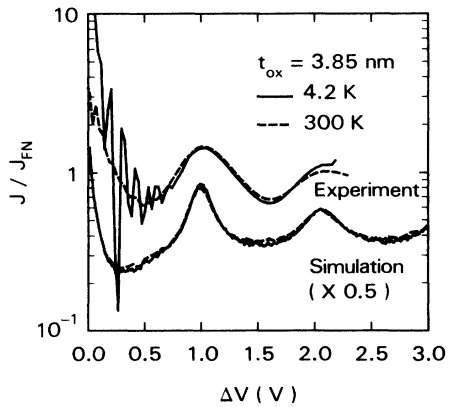

FIG. 5. Experimental and simulated $J/J_{\rm FN}$ ratio at 300 and 4.2 K. The results of the simulation are shifted by a factor 0.5 to help the visualization. The very small temperature dependence is consistent with electron transport dominated by polar scattering with high-energy (0.153 eV) LO phonons. The oscillations observed at low gate voltage at 4.2 K are caused by experimental noise.

in Fig. 3, obtaining as our best estimates the value $m^*=0.5m_0$ (and so $m_{\rm pol}\simeq 0.7m_0$), which agrees very well with previous experimental[6,22] and theoretical[23] results. The fraction of ballistic electrons as a function of the distance x_L traveled in the SiO_2 conduction band in the transient situation of these experiments is shown in Fig. 4. The quasiexponential decay for $x_L < 2$ nm is controlled mainly by polar collisions, while a sharp drop of the number of ballistic electrons is seen as nonpolar collisions take over at electron energies above about 2 eV (Refs. 13 and 14). The dashed line represents a qualitative exponential fit useful to compare our results to those obtained by Lewicki and Maserjian. For the particular data of Fig. 4, we obtain a mean free path of 1.35 nm when fitting the initial portion of the curve. A smaller value ($\lesssim 1$ nm) would be obtained when fitting the full curve. However, this procedure provides somewhat ambiguous values, since the actual mean free path depends—via the electric field and oxide thickness—on the electron energy. Also, a single exponential seems to be a rather crude approximation which we employ only for the sake of comparison with Lewicki and Maserjian's data. Despite this, our results are in satisfactory agreement with their value of 0.65 nm.

A clear indication that at low energy the polar scattering is the dominant collision process was provided indirectly in our previous work[24,25] by the observation that steady-state transport at electric fields below 2×10^6 V/cm (i.e., for average electron energies below 2 eV) behaves as predicted by the older theories based on polar scattering only.[12] Another indication of this fact is provided by the results shown in Fig. 5. Current-voltage characteristics in the tunneling regime at room temperature and liquid-helium temperature exhibit oscillations of very similar amplitude, both experimentally and theoretically. This is expected for collision processes involving high-energy phonons (as the 0.153-eV LO phonons), whose population is little affected by variations of temperature, as long as $k_BT \ll \hbar\omega_{\rm LO}$, k_B being the Boltzmann constant. The application of a magnetic field (Fig. 6) parallel to the interfaces has no effect on the oscillations because of the thinness of the oxide and the high electron velocity.[14]

To conclude this section on the quantum oscillations, we show in Fig. 7 the $J/J_{\rm FN}$ ratios obtained at both polarities in samples with (unannealed) Al (a) and polysilicon (b) gates. Little dependence on bias polarity is seen in samples with polysilicon gates. More interesting is the fact that oscillations are clearly observed even when tunneling from the silicon substrate through the oxide into the aluminum gate. The amplitude of the oscillations due to interference at the Al-SiO_2 interface is strongly reduced with respect to the oscillations originating at the Si-SiO_2 interface. This confirms the widespread belief that oxide-metal interfaces are roughened by chemical reactions occurring at those interfaces.[10] The postmetallization annealing (PMA) usually performed in MOS devices would increase the reaction rate, induce a further roughening of the interface, and damp the oscillations below the limit of observation. Finally, this first observation of quantum interference effects at the oxide-gate in-

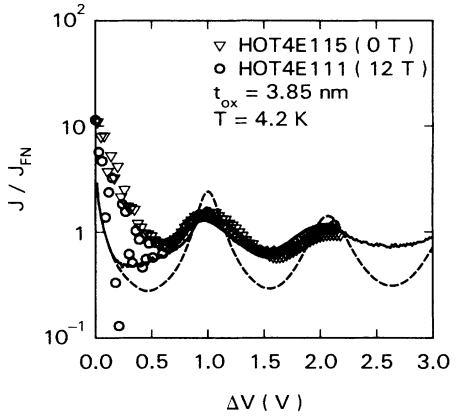

FIG. 6. Experimental $J/J_{\rm FN}$ ratio at 4.2 K with (circles) and without (triangles) the application of a 12-T magnetic field parallel to the SiO_2-electrode interfaces. The simulation (ballistic: dashed line; with inclusion of scattering in the oxide: solid line) is performed at zero field.

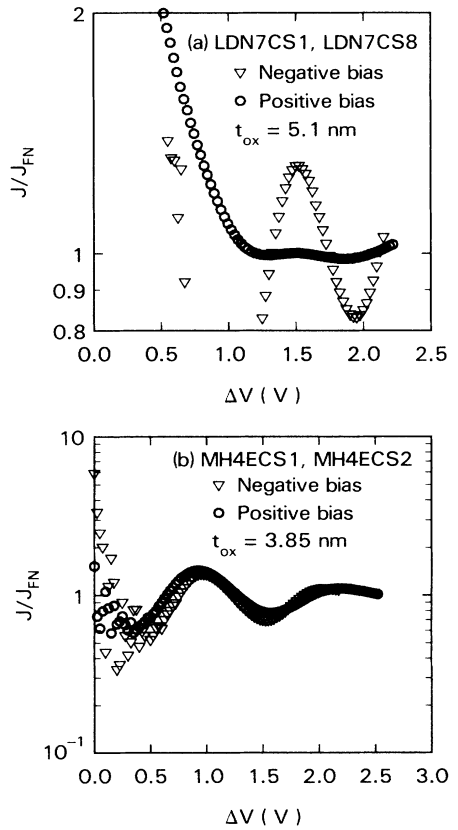

FIG. 7. Quantum oscillations due to interference of the electron wave function at the Si-SiO_2 interface [negative bias in (a) and (b)], at the unannealed SiO_2-Al interface [positive bias in (a)], and at the SiO_2-polysilicon interface [positive bias in (b)]. The amplitude of the oscillation at positive bias in (a) is damped by the roughness of the SiO_2-Al interface.

terface shows very clearly that the density of states (DOS) of the anode material plays little or no role in the modulation of the tunneling current. This is easily understood by noticing that the variation of the DOS of Al or Si over the narrow energy range covered by tunneling measurements is too small to have any significant effect.

III. CARRIER SEPARATION

The observation of the quantum oscillations in the tunneling characteristics of an MOS device is definitely a clear proof of the existence of ballistic electrons in thin SiO_2 layers. However, the information one can extract from these observations is somewhat limited: Experimentally, oscillations can be seen only over a limited range of voltage and oxide thickness. Theoretically, the tunneling problem must be necessarily oversimplified with approximations about the boundary conditions of the wave functions and about the abruptness of the interfaces which limit the overall validity of the simple model leading to Eq. (1).

We have been able to obtain *direct* evidence of ballistic transport in thin oxides by using the same techniques we have employed before to study steady-state transport in thick oxides: the *carrier-separation* and the *vacuum-emission* techniques. Since they have been described at length in previous publications,[7,8] we shall simply recall here and in the next section the type of information they provide, concentrating mainly on the observations relative to ballistic transport.

In *carrier separation,*[7] electrons are injected from the polysilicon gate of a p-channel FET into the gate oxide. As they enter the silicon substrate, electron-hole pairs are generated and the number of pairs can be counted by measuring separately the substrate (electrons) and channel (holes) currents. Using a sufficiently accurate evaluation of the ionization probability in Si as a function of electron energy,[26] it is possible to retrace the average energy the electrons gained in the gate oxide. For ballistic transport, we expect that all electrons should enter the Si substrate with energy $\phi_s + e\,\Delta V$.

In Figs. 8 and 9, we plot the average energy measured by the carrier separation as a function of the voltage applied to the oxide, V_{ox}, from which we have subtracted the voltage drop at the SiO_2-gate interface $\phi_B/e \simeq 3.1$ V, obtaining the quantity ΔV. From the average energy we have subtracted $\phi_s = 3.1$ eV, to obtain the electron kinetic energy in the oxide. Therefore, the solid straight line of unit slope represents the average energy the electrons should have, if all of them could cross the oxide ballistically. As long as $\Delta V \lesssim 1$ eV, this is what we observe experimentally (dashed line) from the carrier separation and from the vacuum emission (shaded region in Fig. 9) which we will describe in the next section. The undulation in the data at about $\Delta V \simeq 0.8$ V might be related to the same quantum oscillations discussed above. In fact, the electrons which attempt to cross the oxide ballistically will be reflected at the Si-SiO_2 interface with probability $1 - P/P_{WKB}$. The average energy will be modulated accordingly. This is seen in the Monte Carlo simulation (dotted line) which includes the quantum reflections in the

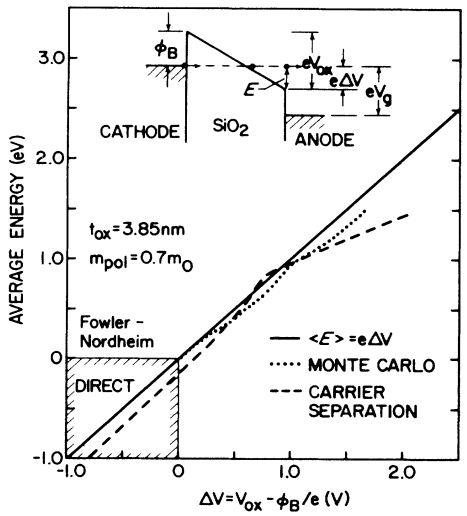

FIG. 8. Average electron kinetic energy in SiO_2 as a function of the voltage ΔV dropping across the distance x_L in the oxide as obtained from the carrier-separation technique in a sample having a 3.85-nm-thick oxide. The solid line would be observed for pure ballistic transport. The results of Monte Carlo simulations including interference effects are also shown.

evaluation of the average energy $\langle E \rangle$:

$$\langle E \rangle = \frac{\sum_i E_i P_i}{\sum_i P_i}\,, \tag{5}$$

where E_i is the energy of the ith electron, and P_i is either the (normalized) transmission probability P/P_{WKB} given

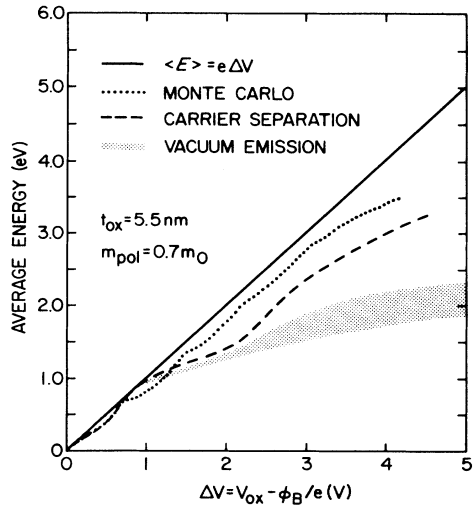

FIG. 9. Average electron kinetic energy in SiO_2 as a function of the voltage drop ΔV as obtained from the carrier separation and from the vacuum-emission techniques in samples having a 5.5-nm-thick oxide. Both thermally grown and plasma-enhanced chemical-vapor-deposited oxides with thicknesses ranging up to 10 nm have been employed in the vacuum-emission experiments.

by Eqs. (1) and (2) for ballistic electrons, or is unity for electrons which have scattered inelastically at least once, thus losing memory of their phases. Destructive interference results in minima of the average energy as a function of ΔV, while the full "ballistic" energy is recovered when constructive interference occurs. While the positions of the maxima and minima of the tunneling current observed experimentally agree extremely well with those predicted theoretically (Figs. 3, 5, 6, and 7), the agreement is far from perfect when looking at the average energies of Figs. 8 and 9. This might be due to the problems we have discussed in Sec. II concerning the use of the "dressed" electron mass, as well as to uncertainties in processing the data, or from the variation of the DOS in the Si substrate used as a "detector" whose efficiency might vary slightly from the one calculated in Ref. 26. The vacuum-emission data we present below (Sec. IV) will add evidence to the oscillating behavior of the ballistic peak and support our interpretation of the undulations of the $\langle E \rangle$-versus-ΔV curves.

At higher applied voltage ($\Delta V > 1.5$ V) (Fig. 9) the average energy drops below the *ballistic line,* approaching the steady-state value. Some uncertainty exists in the experimental data, since the voltage ΔV is obtained from the applied gate voltage corrected for barrier heights and potential drop in the Si, quantities which we can determine with a combined error of about 0.1 eV. However, the Monte Carlo simulation predicts a slower approach to steady state then actually observed. This difference has been consistently obtained even at steady state in the energy range 1 to 2 eV; that is, at the heating threshold.[24,25] The energy distributions we will present in the next section confirm this disagreement which appears to be "real." An obvious reason for the inaccuracy of the Monte Carlo simulation is that, independently of the parameters used, the "intermediate" range of electron energy (1 to 3 eV) is poorly treated. Apart from polaron corrections, we know what the electron effective mass is at the bottom of the SiO_2 conduction band[6,22,23] and we can reasonably assume that the electrons are "almost free" at high energies.[27] We can use the deformation-potential approximation[28] and the rigid-ion approximation[29] to treat the nonpolar electron-phonon collisions at low and high energy, respectively. But in the intermediate range (electrons far from the center and far from the edges of the Brillouin zone) we rely on unjustified interpolations. Moreover, among the various coupling constants employed in the Monte Carlo simulation, the most suspicious appears to be the deformation potential (i.e., the strength of the nonpolar-electron—acoustic-phonon interaction at low electron energy). As we stated in previous publications,[13,14] while we could "guess" the importance of the nonpolar collisions at high electron energies, we simply extrapolated those values to lower energies in an empirical way. Our value for the deformation potential ($\simeq$3.5 eV) is of the same order of the value used by Köster and Hübner,[30] but much smaller than the one employed by Porod and Ferry[31,32] ($\simeq$25 eV). As the situation stands now, neither a suitable choice of a particular value, nor even the inclusion of the Harrison nonpolar-electron—optical-phonon scattering,[33] seems to help in reproducing both the heating threshold[24,25] and the low-field mobility data.[34] To further complicate the issue, density of states and quantum-broadening effects might play some role, as one can see comparing the "golden-rule" rates to the imaginary part of the self-energy employed in the quantum Monte Carlo (QMC) simulation.[35] We could definitely take the "usual" approach and look for a value of the deformation potential which gives the best agreement with the data of Fig. 9. If we were able to account for nonparabolicity, density of states, Harrison interaction, and quantum effects, we would trust the physical meaning of the values we would eventually obtain. Unfortunately, the long computing time needed to solve the Dyson equation and to perform the QMC for every trial value of the coupling constants prevents us from doing so. Therefore, rather than forcing a fit to the data with values of the deformation potential which would carry no physical meaning, we prefer to hold our attempts and wait for additional data on the electron drift velocity at high fields or for an independent determination of the deformation potential from measurements of the SiO_2 structure factor with neutron diffraction experiments or other techniques.

In conclusion, the results of the carrier-separation experiments coupled to the Monte Carlo simulations provide a clear picture of the transient electron transport in thin oxides: Transport occurs in a mostly ballistic regime for the first nanometer traveled by the electrons in the SiO_2 conduction band, up to energies of about 1 eV. The polar electron-phonon collisions slowly reduce the number of ballistic carriers after 2 to 3 nm. Finally, as the electron energies grow above about 2 eV, the nonpolar scattering takes over quickly, driving the electrons towards steady-state. This is observed to occur at a faster rate than predicted by the simulation.

IV. VACUUM EMISSION

Perhaps the most spectacular evidence of ballistic transport can be obtained using the *vacuum-emission* technique.[8] MOS capacitors with thin oxide layers (5 to 10 nm) thermally grown or deposited by plasma-enhanced chemical-vapor deposition (PECVD) on Si substrates of resistivity $\simeq$0.01 Ω cm (for the thermal oxides) to 0.001 Ω cm (for the PECVD oxides) are used to inject electrons from the substrate into the oxide. A thin (12—25-nm) Al gate will collect most of the carriers. But approximately one out of every 10^5 electrons will escape through the metal into the vacuum chamber in which the capacitor is mounted. After being focused, these electrons are energy analyzed by varying the retarding potential $V_{\rm ana}$. Figure 10 shows that, as the retarding potential is reduced, electrons exiting the oxide with energy larger than $\chi + eV_{\rm ana}$ ($\chi \simeq 0.9$ eV being the electron affinity of SiO_2) will be collected. Therefore, if $I_{\rm vac}(E)$ is the current due to the electrons ejected into the vacuum with energy $E \geq \chi + V_{\rm ana}$, the average electron energy can be evaluated using the relationship

$$\langle E \rangle = \frac{\int_0^\infty dE\, I_{\rm vac}(E)}{I_{\rm vac}(0)} \ . \tag{6}$$

Moreover, since

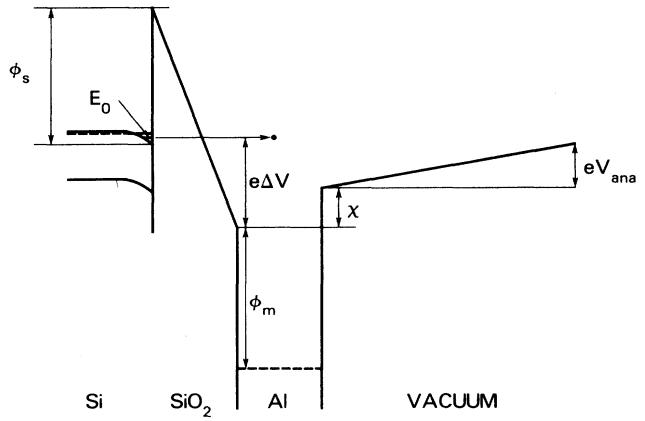

FIG. 10. Schematic diagram illustrating the configuration of the electron potential energy in the vacuum-emission technique.

$$I_{vac}(E)=A\int_E^{\infty} dE'\,n(E')\,, \tag{7}$$

where $N(E)$ is the electron energy distribution, taking the derivative of the vacuum current I_{vac} with respect to the analyzer potential will provide the energy distribution of the electrons. The constant A appearing in Eq. (7) is $eK/\Delta t$, where Δt is the counting (integration) time interval and K is a factor dependent on the efficiency of the Einsel lens system (including the focusing and analyzing sections), on the efficiency of the electron multiplier employed to count the electrons, and on the emission efficiency of the device. (Being very difficult to evaluate *a* priori the overall efficiency K, the experimental results obtained from the vacuum-emission experiments are defined up to an arbitrary multiplicative constant.) Thus, the vacuum-emission technique allows a direct observation of the ballistic peak of electrons in the energy distribution.

Several experimental problems should be pointed out. In the first place, electrons having kinetic energy smaller than the SiO_2 electron affinity χ ($\simeq$0.9 eV) cannot be observed. Double metallization schemes which we employed previously[8,25] in thick oxides did not exhibit the "cesiating" effect we had expected. Perhaps because of the different stress conditions associated with the thin SiO_2 films, the deposition of thin Au films resulted in nonuniform coverage with areas of the device over which the metal had actually lifted off. Thus, only relatively highly energetic electrons could be observed. Since ballistic transport occurs only over the first couple of nm of oxide, we had to compress our observations over a very narrow range of oxide thickness: Thinner oxides had to be driven at unbearable current levels ($\gtrsim 10^{-2}$ A/cm^2) and field strengths ($\gtrsim 10^7$ V/cm) for relatively large periods of time (of the order of minutes), while thicker oxides would show distributions approaching steady state and not the ballistic electrons we are interested in. The range 5.1 to 5.8 nm—corresponding to a distance traveled by the electrons in the SiO_2 conduction band of about 1 to 3 nm at the fields we have employed—was actually the useful operating range. Breakdown problems remain serious, since we want to avoid the use of Si-rich—SiO_2 injectors[36] over which a significant—and difficult to evaluate—voltage drop would occur. Very carefully designed growth and annealing sequences had to be employed to obtain thin films of thermally grown[37] or PECVD-deposited SiO_2 layers[38] which could withstand the high current levels and fields for a long time.

A second problem is due to the fact that thin gate electrodes had to be used in the attempt to minimize the broadening of the electron distributions due to electron-electron scattering in the metal. Combined with the high fields used in the experiments, this results in very large vacuum emission currents. Unfortunately, the efficiency of the multiplier affecting the constant A of Eq. (7) is constant up to about 2×10^5 counts/sec, decreasing rapidly at higher counts. Thus, data obtained at very large gate and vacuum-emission currents are unreliable. This further restricts the energy range we can analyze. In Fig. 11, we show how we can simultaneously verify the linearity of the multiplication efficiency and determine the work function of the metal gate. For every device, we fix the analyzer voltage at $V_{ana}=0.8$ V (to compensate for the Al-gate—Au-analyzer contact potential difference) and then increase the gate voltage. Assuming that the electrons tunnel from the highest occupied subband in the accumulation layer of the Si substrate with energy E_0 (<0) below the Fermi level in the cathode and reach the vacuum ballistically, we expect the electron counts to increase with the gate voltage V_G as

$$\begin{aligned} I_{vac}(V_G) &\propto T(E_T=E_0, V_G)\int_{E_0}^{eV_G-\phi_m-\chi} dE\,\rho_2(E)f(E) \\ &\propto T(E_T=E_0, V_G)(eV_G-\phi_m-\chi-E_0)\,, \end{aligned} \tag{8}$$

where $\rho_2(E)$ is the two-dimensional density of states in the accumulation layer, E_T is the "transverse electron energy" in Si defined as $\hbar k_T^2/2m_s$, k_T being the quantized com-

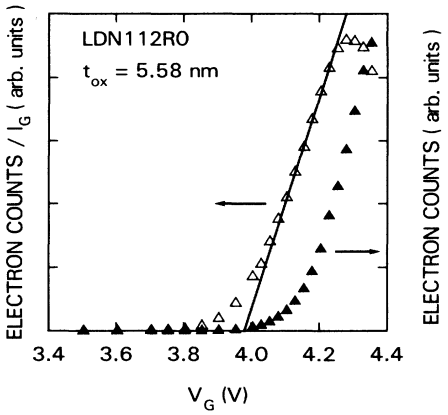

FIG. 11. Electron counts vs gate voltage (solid triangles) and electron counts normalized by the gate current I_G vs gate voltage (open symbols) in the vacuum-emission experiment for a device having a 5.58-nm-thick oxide and a 15.5-nm-thick Al gate. Loss of ballistic behavior would result in a flattening of the curve counts/I_G vs V_G. The observed decrease of the curve implies saturation of the electron multiplier.

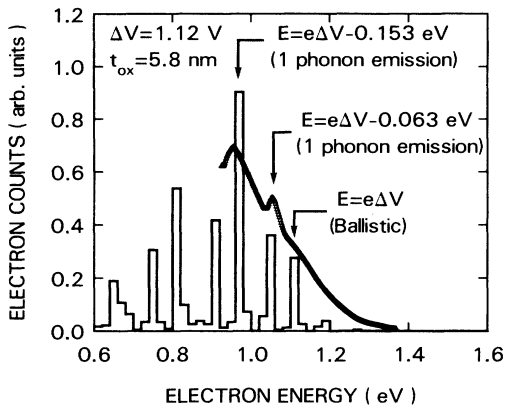

FIG. 12. Experimental electron energy distribution obtained from the vacuum-emission experiments (small triangles) and results of a Monte Carlo simulation (histogram) showing the ballistic peak and the side bands associated with electrons which have emitted one low-energy or one high-energy LO phonon. The thickness of the thermal oxide film is 5.8 nm, while the Al gate is 21.2 nm thick.

ponent of the electron wave vector normal to the Si-SiO_2 interface, and $T(E_T,V_G)$ is the tunneling probability for an electron of "transverse" energy E_T at bias V_G. In deriving the last member of Eq. (8), we have ignored the tail of the Fermi function $f(E)$ responsible at nonzero temperature for the soft threshold of Fig. 11. Thus, if we monitor the electron counts as the gate voltage increases, and divide them by the total current [proportional to $T(E_0,V_G)$], we should obtain a straight line intercepting the abscissas at $eV_G=\phi_m+\chi+E_0$. Typical values for this threshold range from 3.95 to 4.05 V (as in the example illustrated in Fig. 11). Deviation from linearity can be seen above $V_G \gtrsim 4.2$ V, corresponding to about 2×10^5 counts/sec. We attribute this deviation to electrons beginning to lose their ballistic behavior as well as to saturation phenomena of the electron multiplier. We shall present only data which are unaffected by this latter problem.

A final problem concerns the paths followed by those electrons which escape the metal gate and are ejected into the vacuum. In the past, we have argued the voids (or "pinholes") in the metal are most likely responsible for the large fraction of escaping electrons.[8,25] Definitely, the metal behaves far from ideally in stopping the electrons since, for instance, the counts drop far too slowly as the metal is made thicker. Lensing effects close to voids are excluded by the independence of the heating threshold on applied voltage for increasing oxide thickness.[24,25] In the course of the present experiments, we also observed—as we shall stress below—that the distributions we obtained are consistent with a ballistic peak whose amplitude is modulated ideally by the quantum interference at the SiO_2/ anode interface. This would not occur if the electrons scattered in the metal. Our present understanding is that at the edges of the voids the oxide surface is covered by much thinner metal regions—compared with the nominal metal thickness—which are likely to be almost transparent to the electrons. Electrons hitting thicker regions of the metal are collected as gate current. Since there are no field lines terminating in the void regions, no carriers can be emitted there. Unfortunately, we miss a better understanding of this issue. It would be particularly helpful to understand the role of the metal in broadening the electron distributions, in view of the erratic broadening we have observed moving from one sample to another. Undoubtedly, poorly controlled details of the metal layer at the levels of single grains might affect the measurement. This was not a serious problem in our previous experiments since we were dealing with energies and distribu-

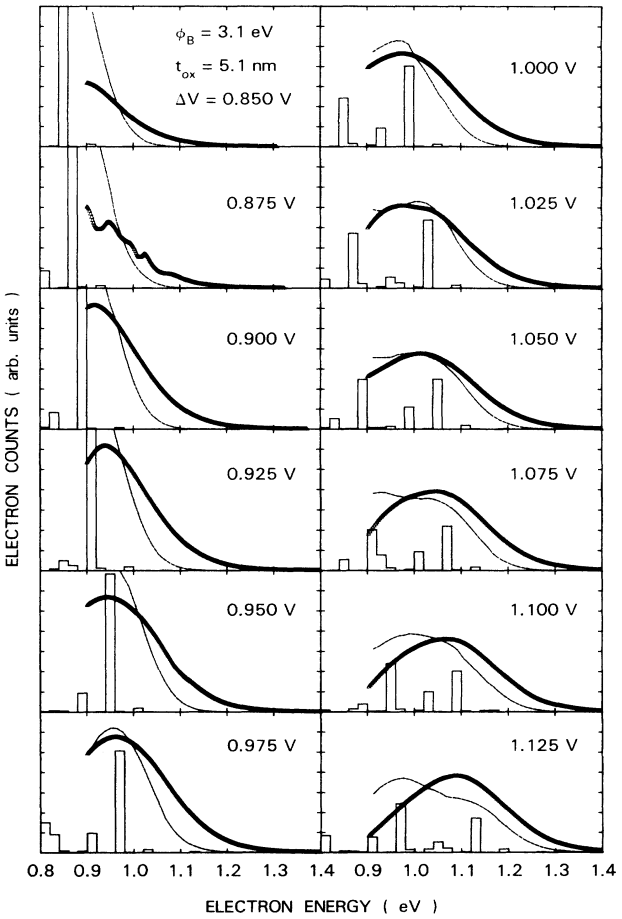

FIG. 13. Experimental electron energy distributions obtained from the vacuum-emission technique (thick lines of small symbols) compared to results of the Monte Carlo simulations (histograms). The dashed lines are obtained by broadening the Monte Carlo results with a Gaussian of 75 meV half width at half maximum. Notice the appearance of the ballistic peak as the voltage drop ΔV increases and its decay with the simultaneous appearance of the phonon replicas. The ballistic peak must be modulated by the quantum interference effects to obtain good agreement with the data. The experimental distributions as functions of bias voltage are normalized by dividing the electron counts at a given ΔV by the gate current at the same bias. This normalization is correct only to within 20%. The thermal oxide is 5.1 nm thick, while the Al gate is 12 nm thick.

tions in the eV range. It appears more serious in the present context, since we analyze distributions requiring a resolution in the 0.1-eV range or better.

We show in Fig. 12 the most striking result of our investigation: Not only a clear "shoulder" is observed at the energy expected for the ballistic electrons, but phonon replicas are clearly observed. The narrow peaks correspond to electrons which have traveled about 2.7 nm in the SiO_2 conduction band by emitting one LO phonon of energy 0.063 or 0.153 eV. The Monte Carlo simulation agrees not only in predicting the position of the peaks, but also in predicting their relative height. Notice that the ballistic peak had to be damped by the factor P/P_{WKB}, implying a sharp potential discontinuity at the SiO_2-anode interface (at least over the area which emits electrons). To our knowledge, this is the most direct verification of the electron-lattice interaction strength that has ever been provided. We should remark that many factors contributed in making the observation possible; among them: the oxide thickness in the right "window," the metal thickness small enough to have a limited effect on the width of the peaks, and the thermal oxide carefully prepared so that long integration times Δt could be used to reduce the noise of the data. The observation has been repeated on the same sample and on other samples of the same wafer. Also, several different smoothing algorithms have been employed to evaluate the numerical derivative of the raw data and to ensure that no artifacts were introduced by the cubic spline fitting, often responsible for spurious oscillations.

We conclude by presenting in Figs. 13 through 16 four sequences of electron energy distributions as the gate voltage is varied. In all sequences the shift and modulation of the ballistic peak is clearly visible. Simultaneously, phonon replicas at lower energy appear. Although the fine structure we observed in the sample shown in Fig. 12 is not always reproduced, shoulders do appear in the experimental distributions which are well correlated with the peaks of the Monte Carlo simulation. To better check the consistency of the experiments with the theory, we have broadened the simulation with a Gaussian of 75-meV half width at half maximum. This empirical broadening is of the order of magnitude which must be expected from various contributions, such as the electron scattering in

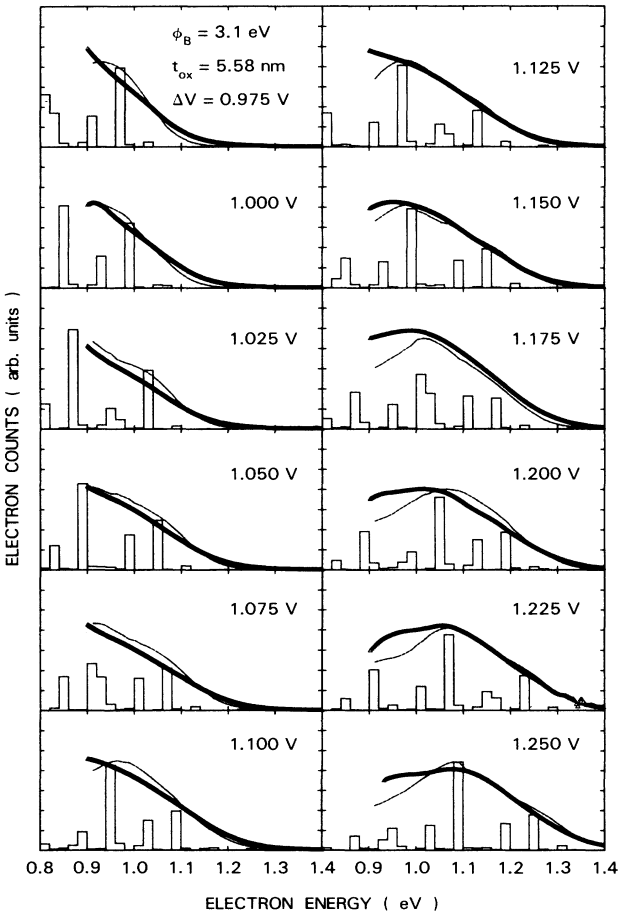

FIG. 14. A sequence of electron energy distributions and Monte Carlo simulations as in Fig. 13 for a thermal oxide 5.58 nm thick and an Al gate 15.5 nm thick.

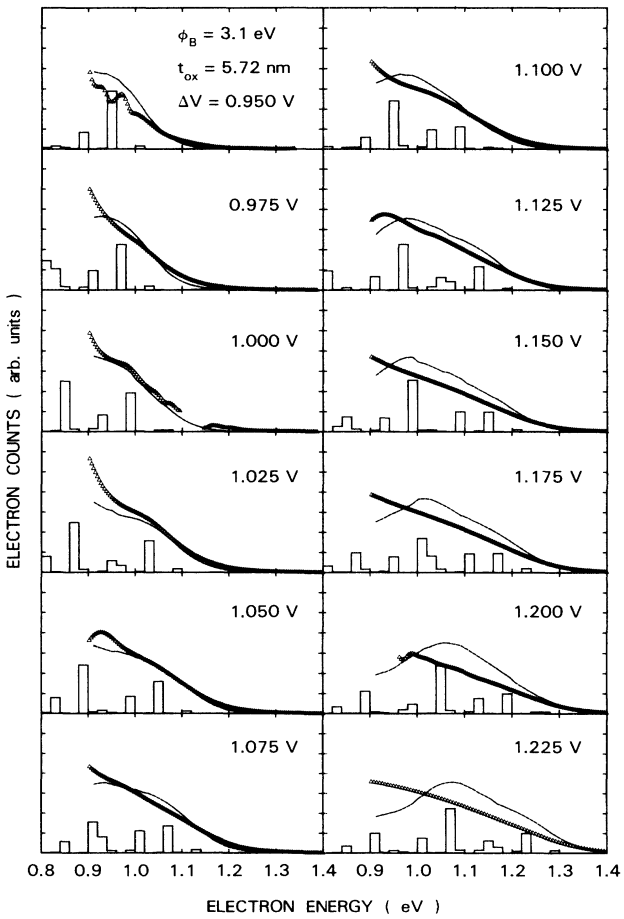

FIG. 15. A sequence of electron energy distributions and Monte Carlo simulations as in Fig. 13 for a thermal oxide 5.72 nm thick and an Al gate 15.5 nm thick.

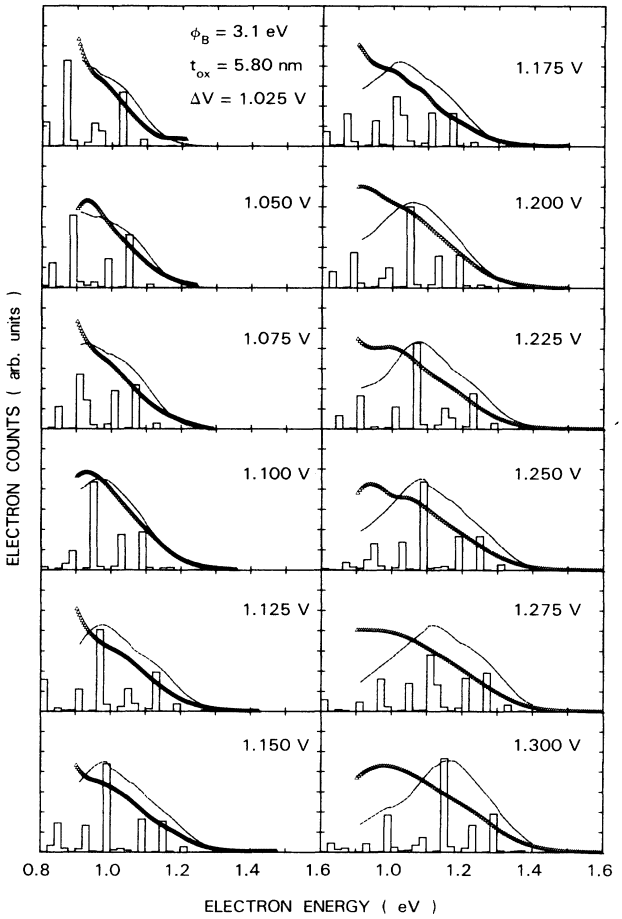

FIG. 16. A sequence of electron energy distributions and Monte Carlo simulations as in Fig. 13 for a thermal oxide 5.8 nm thick and an Al gate 21.2 nm thick. At large biases ($\Delta V \gtrsim 1.2$ V) the Monte Carlo simulation predicts a slower thermalization than is actually observed, as discussed in the text, Sec. III.

the metal, the intrinsic broadening of the electron energy due to the polar collisions,[39] the finite width of the electron distribution entering the oxide conduction band, the energy resolution of the analyzing system, and, possibly, the broadening of the phonon energy which we should expect for noncrystalline SiO_2 (Ref. 20). Finally, the data of Fig. 16 at the highest biases show the reappearance of the disagreement between experiment and simulation we noted in the preceding section. The role of the nonpolar scattering seems much stronger than our deformation potential implies, with the electron distribution being smeared out faster then predicted.

V. CONCLUSIONS

We have shown the existence of ballistic transport in thin films of SiO_2 not only deducing it *indirectly* from the quantum oscillations in the tunneling current-voltage characteristics, but observing the ballistic carriers *directly* using the carrier-separation and the vacuum-emission techniques. These are not the first observations of ballistic transport in solids. We consider Lewicki and Maserjian's original work[6] as the first indirect evidence of the phenomenon, while direct evidence has been already provided using GaAs-based devices.[1,2] However, the observations we reported are the most direct check of the electron-lattice interaction ever provided, thanks to the almost ideal behavior of thermally grown SiO_2 and to the weakness of the electron-electron interaction in our experiments. Whether ballistic transport will ever find an application to real devices or not, experiments of this type, coupled to theoretical simulations, can give us information about the properties of electronic transport in solids almost at the atomic level.

We have not addressed the fundamental issues concerning the tunneling process: How fast does the electron become a small polaron? Is phase coherence preserved as the polarons are being formed? How do quantum interference phenomena affect the electron transit and tunneling time? Is one single collision process sufficient to randomize completely the phases of the electrons and destroy the coherence effects? The simple-minded approximations we have employed in our Eqs. (1), (3), and (5) seem to explain the data in a satisfactory way. But the basic problems under these approximations remain unsolved.

One of the surprises of our work is certainly the *too ideal* behavior of thermally grown SiO_2. The phonon replicas observed in a few samples are as narrow as 50 meV, their height predicted in an excellent way by simulations which treat the oxide as an ideal crystal. In the past, structural studies of thermal SiO_2 layers have led several investigators to conclude that the thermal oxidation of silicon produces a form of oxide which is not totally amorphous. Rather, a short-range order over the scale of 3 nm or so could explain many of its properties.[40] Our results give additional support to this idea, showing insignificant broadening of the LO-phonon energy—consistent with the ideas of Ref. 20—and absence of additional scattering mechanisms related to the possible disorder of the structure. This lucky circumstance not only renders SiO_2 a vital insulator in the present technology but, paradoxically, makes it the best understood material as far as electronic conduction is concerned.

ACKNOWLEDGMENTS

We would like to thank A. B. Fowler for many conversations on the basic physics of the quantum effects involved in elastic and inelastic tunneling, M. H. Brodsky, A. B. Fowler, J. R. Kirtley, F. Stern, and T. N. Theis for having critically read the manuscript.

[1]J. R. Hayes, A. F. J. Levi, and W. Wiegmann, Phys. Rev. Lett. **54**, 1570 (1985); Appl. Phys. Lett. **47**, 964 (1985).

[2]M. Heiblum, M. I. Nathan, D. C. Thomas, and C. M. Knoedler, Phys. Rev. Lett. **55**, 2200 (1985); M. Heiblum, D. C. Thomas, C. M. Knoedler, and M. I. Nathan, Appl. Phys. Lett. **47**, 1105 (1985).

[3]A. F. J. Levi, J. R. Hayes, P. M. Platzmann, and W. Wiegmann, Phys. Rev. Lett. **55**, 2071 (1985).

[4]A. F. J. Levi, J. R. Hayes, and R. Bhat, Appl. Phys. Lett. **48**, 1609 (1986).

[5]D. J. DiMaria, M. V. Fischetti, J. Batey, L. Dori, E. Tierney, and J. Stasiak, Phys. Rev. Lett. **57**, 3213 (1986).

[6]G. Lewicki and J. Maserjian, J. Appl. Phys. **46**, 3032 (1975).

[7]D. J. DiMaria, T. N. Theis, J. R. Kirtley, F. L. Pesavento, D. W. Dong, and S. D. Brorson, J. Appl. Phys. **57**, 1214 (1985).

[8]S. D. Brorson, D. J. DiMaria, M. V. Fischetti, P. M. Solomon, and D. W. Dong, J. Appl. Phys. **58**, 1302 (1985).

[9]K. H. Gundlach, Solid-State Electron **9**, 949 (1966).

[10]J. Maserjian and N. Zamani, J. Appl. Phys. **53**, 559 (1982).

[11]In Ref. 6 the argument was made that interference could be seen only for electrons traveling back and forth twice in the SiO_2 conduction band over the distance x_L defined in the text following Eq. (1) and in Fig. 2. Thus, the mean free path was obtained by plotting the amplitude of the oscillations versus $2x_L$. This is not the correct procedure, since interference occurs by summing over the infinitely many reflections of plane waves which are automatically included in the solution of the time-independent Schrödinger equation with the proper boundary conditions. In a time-dependent problem, once steady state is reached, the situation would not change, provided the electron has a well-defined energy so that the eigenpacket associated with it is sufficiently well localized in k space. Thus, the amplitude of the oscillations should be plotted as a function of x_L only and the mean free path obtained in Ref. 6 (1.3 nm) should be divided by a factor of 2.

[12]See, for instance, T. H. DiStefano and M. Shatzkes, Appl. Phys. Lett. **25**, 685 (1974); P. Solomon and N. Klein, Solid State Commun, **17**, 1397 (1975); D. K. Ferry, Appl. Phys. Lett. **27**, 689 (1975).

[13]Massimo V. Fischetti, Phys. Rev. Lett. **53**, 1755 (1984).

[14]M. V. Fischetti, D. J. DiMaria, S. D. Brorson, T. N. Theis, and J. R. Kirtley, Phys. Rev. B **31**, 8124 (1985).

[15]See, for instance, A. S. Davydov, *Quantum Mechanics* (Pergamon, London, 1965), p. 80.

[16]E. De Castro and P. Olivo, Phys. Status Solidi B **132**, 153 (1985), and references therein.

[17]R. J. Powell, J. Appl. Phys. **41**, 2424 (1970).

[18]Tsuneya Ando, Alan B. Fowler, and Frank Stern, Rev. Mod. Phys. **54**, 437 (1982), p. 485 ff.

[19]W. T. Lynch, J. Appl. Phys. **43**, 3274 (1972).

[20]Klaus Hübner, in *The Physics of MOS Insulators,* Proceedings of the International Topical Conference, Raleigh, North Carolina, 1980, edited by Gerald Lucovsky, Sokrates T. Pantelides, and Frank L. Galeneer (Pergamon, New York, 1980), p. 82.

[21]See, for instance, C. Kittel, *Quantum Theory of Solids* (Wiley, New York, 1963), p. 141.

[22]Z. A. Weinberg, J. Appl. Phys. **53**, 5052 (1982).

[23]James R. Chelikowsky and M. Schlüter, Phys. Rev. B **15**, 4020 (1975).

[24]D. J. DiMaria, M. V. Fischetti, E. Tierney, and S. D. Brorson, Phys. Rev. Lett. **56**, 1284 (1986).

[25]D. J. DiMaria, M. V. Fischetti, M. Arienzo, and E. Tierney, J. Appl. Phys. **60**, 1719 (1986).

[26]R. C. Alig, S. Bloom, and C. W. Struck, Phys. Rev. B **22**, 5565 (1980).

[27]M. Sparks, D. L. Mills, R. Warren, T. Holstein, A. A. Maradudin, L. J. Sham, E. Loh, and D. F. King, Phys. Rev. B **24**, 3519 (1981).

[28]J. Bardeen and W. Shockley, Phys. Rev. **80**, 72 (1950).

[29]J. M. Ziman, *Principles of the Theory of Solids* (Cambridge University Press, Cambridge, 1972), p. 205.

[30]H. Köster, Jr. and K. Hübner, Phys. Status Solidi B **118**, 293 (1983).

[31]W. Porod and D. K. Ferry, Phys. Rev. Lett. **54**, 1189 (1985).

[32]W. Porod and D. K. Ferry, in Proceedings of the 4th International Conference on Hot Electrons in Semiconductors, Innsbruck, Austria, 1985, edited by E. Gornik [Physica B (to be published)].

[33]W. A. Harrison, Phys. Rev. **104**, 1281 (1956).

[34]R. C. Hughes, Phys. Rev. Lett. **26**, 1933 (1973); Phys. Rev. B **15**, 2012 (1977); Solid-State Electron **21**, 251 (1978).

[35]Massimo V. Fischetti and D. J. DiMaria, Phys. Rev. Lett. **55**, 2475 (1985).

[36]S. Yokoyama, D. W. Dong, D. J. DiMaria, and S. K. Lai, J. Appl. Phys. **54**, 7058 (1983).

[37]M. Arienzo, L. Dori, and T. N. Szabo, Appl. Phys. Lett. **49**, 1040 (1986).

[38]J. Batey and E. Tierney, J. Appl. Phys. **60**, 3136 (1986); J. Batey, E. Tierney, and T. N. Nguyen, IEEE Electron Dev. Lett. (to be published).

[39]The so-called "collisional broadening" is discussed by F. Capasso, T. P. Pearsall, and K. K. Thornber, IEEE Electron Device Lett. **EDL—21**, 295 (1981) and implemented in Monte Carlo simulations by Yia-Chung Chang, D. Z.-Y. Ting, J. Y. Tang, and K. Hess, Appl. Phys. Lett. **42**, 76 (1983).

[40]This point has been discussed recently in the review article by Frank J. Feigl, Physics Today, **30**(10), 47 (1986).